Mechanical impact stimulation platform tailored for high-resolution light microscopy

ORIGINAL PAPER

Mechanical impact stimulation platform tailored for high-resolution light microscopy

Heidi T. Halonen[1] · Jari A.K. Hyttinen[1] · Teemu O. Ihalainen[2]

Abstract

High frequency (HF) mechanical vibration has been used in vitro to study the cellular response to mechanical stimulation and induce stem cell differentiation. However, detailed understanding of the effect of the mechanical cues on cellular physiology is lacking. To meet this limitation, we have designed a system, which enables monitoring of living cells by high-resolution light microscopy during mechanical stimulation by HF vibration or mechanical impacts. The system consists of a commercial speaker, and a 3D printed sample vehicle and frame. The speaker moves the sample in the horizontal plane, allowing simultaneous microscopy. The HF vibration (30–200 Hz) performances of two vehicles made of polymer and aluminum were characterized with accelerometer. The mechanical impacts were characterized by measuring the acceleration of the aluminum vehicle and by time lapse imaging. The lighter polymer vehicle produced higher HF vibration magnitudes at 30–50 Hz frequencies than the aluminum vehicle. However, the aluminum vehicle performed better at higher frequencies (60–70 Hz, 90–100 Hz, 150 Hz). Compatibility of the system in live cell experiments was investigated with epithelial cells (MDCKII, expressing Emerald-Occludin) and HF (0.56 G_{peak}, 30 Hz and 60 Hz) vibration. Our findings indicated that our system is compatible with high-resolution live cell microscopy. Furthermore, the epithelial cells were remarkable stable under mechanical vibration stimulation. To conclude, we have designed an inexpensive tool for the studies of cellular biophysics, which combines versatile in vivo like mechanical stimuli with live cell imaging, showing a great potential for several cellular applications.

Keywords HF vibration · In vitro mechanical stimulation · Live cell imaging · Mechanical impacts · Mechanobiology · Real-time imaging

1 Introduction

Traditionally, cell biological studies are conducted in static cell culture conditions. However, this does not reflect the complex in vivo conditions of cells. In tissues the cells experience varying dynamic mechanical stimuli [1–3] and they are able to sense and adjust their functions accordingly (mechanotransduction) [4, 5]. As an example, epithelial cells experience stretching [6, 7] and mechanical impacts as a result of locomotion [2]. Furthermore,

they are exposed to high frequency (HF, ≥10 Hz) vibration in larynx due to phonation [8]. Therefore, cell culture methods implementing mechanical stimulation would be highly beneficial both for disease modeling and tissue engineering. In addition, details of the cellular force sensing machinery are still poorly understood. Consequently, novel techniques are needed for studying of the mechanical stimulation effects on cells.

The mechanical HF vibration has been applied to cell cultures with the aim to mimic the mechanical environment of cells in vivo [9–16]. The mechanical impact effects on cells, to our best knowledge, have not yet been tested, despite that they could potentially be more in vivo like for many cell types. Both stimulation techniques allow dynamic mechanical stimulation of cell population without directly deforming extracellular matrix surrounding the cells. In the stimulation the cell culture is often moved either in parallel (i.e. vertical HF vibration) [9, 11, 13–15, 17] or perpendicularly (i.e. horizontal HF vibration) [10, 12, 18] to the direction of gravity. Also, simultaneous vertical and horizontal HF vibration (i.e. vertically

✉ Heidi T. Halonen
heidi.halonen@tuni.fi

1 Computational Biophysics and Imaging Group, Faculty of Medicine and Health Technology, Tampere University, 33520 Tampere, Finland

2 Cellular Biophysics Group, Faculty of Medicine and Health Technology, Tampere University, 33520 Tampere, Finland

rotating HF vibration) [19] and combination of the HF vibration with other types of mechanical stimuli, such as stretching [20], compression [21], and fluid shear [22], have been introduced. Different actuators cover a wide vibration frequency range even up to 1 kHz [11, 12, 17]. The vibration magnitudes instead, have most commonly been less than 1 G_{peak}, resulting in low magnitude and high frequency (LMHF) vibration [10–12, 14, 19]. However, also high magnitude and high frequency (HMHF, $\geq 1 G_{peak}$) vibration has been used [9, 10, 12]. In addition to these vibration parameters, adequate rest periods between the stimulation bouts have been shown important for the directing effects of the HF vibration on cell differentiation [23].

Both the HF vibration and the mechanical impact stimuli allow combination of different biochemical stimuli [9] and cell culture materials [24, 25] to large variety of the vibration parameters described above. However, the current understanding on how the HF vibration influences cellular physiology via mechanotransduction processes is only limited. Uzer and co-workers have shown that the vibration magnitude and frequency can influence the balance between the inertial force -related movement of cell nuclei and fluid shear experienced by the cell [10, 18]. Thus, changes in the vibration parameters can lead into altered mechanical stimuli imposed to the cells. Moreover, the same research group provided evidence that the cellular response to the HF vibration is dependent on the intact linkage of the cell nuclei and the actin cytoskeleton through Linker of Nucleoskeleton and Cytoskeleton (LINC) complex [36]. Nevertheless, the current understanding of the downstream effects of HF vibration stimulus on the cellular physiology has been conducted only with the stimulation systems lacking real-time imaging of the cellular response. Moreover, best to our knowledge, mechanosensitivity of the epithelial cells to the HF vibration has not yet been investigated, regardless that these cells respond both to mechanical stretching [26, 27] and fluid shear stress [28, 29].

Originally, Holdsworth and colleagues introduced a device for live cell imaging of the horizontal HF vibration responses in ambient conditions [30]. We recently introduced a miniaturized 3D printed system compatible with most of the inverted light microscopes [31]. Our goal was to develop a stimulation platform for mechanobiology studies, which enables HF vibration and imaging of living cells under temperature and CO_2 controlled conditions on a light microscopy system. In this paper, we characterize the system performance in producing HF vibration by comparing the accelerometer data to sample vehicle movements. In addition, we studied the system performance in producing mechanical impacts by comparing the acceleration data of the aluminum vehicle with time lapse imaging data of the sample movement (gold (Au) -printed line on glass coverslip). Finally, we studied the effect of LMHF vibration on the epithelial cell morphology to show

compatibility of our platform for live cell studies and to provide novel findings of the HF vibration effects on epithelial cells.

2 Material and methods

We set several special requirements for the stimulation platform to make it compatible for the dynamic mechanical stimulation of living cells and their high-resolution light microscopy (Table 1). In brief, the platform must combine horizontal mechanical HF vibration or impacts, time lapse imaging and sample incubation. The designed graphical user interfaces (GUIs) must be user-friendly, providing the user the flexibility to adjust the produced sample vehicle movement in addition to the recording. Our aim was to develop an experimental setup, which enables the analysis of the mechanical stimulation effects on living cells.

2.1 Stimulator design and working principle

The stimulation platform design and working principle have been described in our recent paper [31]. In brief, a microscope stage adapter (stainless steel, m = 451.89 g) was designed to be placed on a well plate adapter of a commercial microscope stage of a laser scanning confocal microscope (e.g. ZEISS LSM 780 LSCM on inverted Cell Observer microscope body, Carl Zeiss AG, Germany) (Fig. 1a). Sample vehicles (acrylonitrile butadiene styrene (ABS), m = 16.01 g; and aluminum, m = 38.65 g) were designed to accept commercial imaging chamber (SC15022, Ø 35.6 mm, m = 40.44 g, Aireka Cells, China), on which a coverslip (22 × 22 mm, Carl Zeiss AG) either with the Au-printed line sample or the sample consisting of living cells emitting fluorescence was mounted. Both the microscope stage adapter and the sample vehicles were manufactured with 3D printing (i.materialise, Netherlands). The sample vehicles were attached to a commercial speaker (ø = 5 cm, Partco Oy, Finland) to move the sample on the microscope stage adapter. Smooth sample movement was enabled by supportive plates and miniaturized wheels (H0e, Roco, Germany), which were added on both sides of the vehicles. Mechanical resonances of the movement were prevented with rubber sheets, glued (Loctite Super Glue Precision, Germany) on the sliding surface of the microscope stage adapter and on the vehicle surfaces. Environmental temperature and CO_2 content of the sample was controlled with a simple sample cover and the microscope system (Incubator XL S1, ZEISS LSM 780 LSCM) and its user interface (Zen Black, Carl Zeiss AG) (Fig. 1b). We designed two stimulator GUIs with LabVIEW (National Instruments, USA) and installed them on a laptop (Lenovo ×220 Thinkpad, Hong Kong) to set the stimulation protocols either for the HF vibration (HF vibration GUI) or mechanical impacts (Mechanical

Table 1 Requirements for the dynamic mechanical stimulation platform

Stimulation platform	Graphical user interface
- mechanically robust, easy and fast to use	- continuous HF vibration: magnitude, frequency, stimulation duration and refractory periods
- applicable in commercial microscope stages	- mechanical impact: magnitude, frequency, and stimulation duration, refractory periods, stimulation direction and waveform
- sterilizable, low weight vehicle compatible with regular-sized petri dish	- 3-axis acceleration visualization and recording
- temperature and CO_2 controls enabled with minimized contamination risk	- minimal user involvement required

impact GUI). These GUIs were used to feed the AC voltage to an audio amplifier (Pro-Ject Amp Box S, PRO-JECT AUDIO SYSTEMS, Austria) through a data acquisition module (DAQ, NI USB-6211, National Instruments) and to real-time monitor the accelerometer-measured sample vehicle movement (3-axis, ADXL325, Analog devices, USA) in time domain and in frequency domain (power spectral density (PSD) estimate). The same stimulator GUIs were used to record the acceleration signals for further analysis. The samples were imaged (C-Apochromat 63 × objective/1.20 W Korr M27, Carl Zeiss AG, Germany) with a differential interference contrast (DIC) light and reflected (Au-printed line) or fluorescence (living cells) lights either during the sample movement (technical tests) or immediately after the stimulation bouts.

## 2.2 Technical tests

2.2.1 HF vibration performance range

Performance of the stimulation platform in producing the sinusoidal HF vibration was evaluated, similarly to in our previous study performed with the aluminum vehicle [31]. In brief, frequency range of 30–200 Hz was tested with the aluminum and ABS vehicles. At the beginning of the test, the large incubator chamber of the microscope (Incubator XL S1) and the stimulation platform were preheated up to 37 °C at least for 20 minutes. The HF vibration GUI was used, when the three-axis accelerations (ADXL325) of the sample vehicles were measured to determine the performance limit of the system. The maximum G_{peak} vibration magnitude was reached, when the measured acceleration of the intended main axis movement (y-axis) did not increase with the increasing AC input voltage of the speaker or the vibration magnitudes in off main axis movement directions (x-axis, z-axis) exceeded 0.5 G_{peak}. The acceleration data was recorded at a sampling frequency (X Ch, Y Ch, Z Ch; f_s = 10 kHz), after which it was analyzed with a matlab-script (MATLAB R2014a (32-bit), MathWorks, MA, USA) that we wrote to analyze the time domain and PSD estimates of the acceleration signals.

2.2.2 Production of mechanical impact stimuli

Accuracy and precision of the stimulation platform in producing mechanical impacts was tested with the aluminum vehicle as described in our previous paper with the LMHF vibration [31]. We used the mechanical impact GUI to set the stimulation protocol, which consisted of 14–15 mechanical impacts, produced at increasing waveform periods (from 1/2 T up to 4/4 T) of sinusoidal, square or triangular waves applied at 5 Hz frequency. In addition, the stimulation direction was altered by changing the polarity of the AC input voltage. The ADXL325-measured acceleration signals were observed and recorded (X Ch, Y Ch, Z Ch; f_s = 3333 Hz) and accuracy and precision of the mechanical impacts were analyzed from the time domain acceleration signals, as described above with the HF vibration performance range.

The mechanical impacts were further evaluated by confocal microscopy imaging of the sample movement (ZEISS LSM 780 LSCM in a Cell Observed microscope body and C-Apochromat 63 × objective/1.20 W Korr M27) simultaneously with the acceleration measurement. The sample was a glass coverslip (15 × 15 mm, Carl Zeiss AG) with a thin reflecting line, constructed lithographically from Au (length = 1 cm, width = 8.5 μm). The Au -printed line movement during the stimulation protocol was recorded by time lapse imaging with high frame rate (17.71 s, frame rate: 286 FPS) of a thin scanning region (512 × 2 px, 134.95 × 0.53 μm) using 488 nm laser line. The reflected light (detection band λ = 479–499 nm) and DIC channel were collected and were analyzed with ImageJ (Fiji package, https://fiji.sc/). The brightness and contrast of the time lapse was first adjusted, after which it was converted to a montage with the aim to compare the effects of mechanical impacts during the stimulation protocols. The first and the last images of the mechanical impacts were used to quantitatively evaluate the stability of the Au -printed line movement in the y-axis (μm). The location of the Au -printed line was measured from the edge of the microscope field of view after which the stability was determined as the distance ratio (%) of the last and first mechanical impacts ($Ratio_{Last/First}$). In addition, the morphology of the Au-printed line movement during the mechanical

Fig. 1 Stimulation system setup (**a**) representative images of the samples, the assembled imaging holder and the designed stimulation platform, consisting of the microscope stage adapter and the supportive structures to produce the horizontal movement of the sample vehicle, scale bars 20 μm (**b**) representative image of the stimulation experiment setup and a blow-up image of the stimulation platform on the microscope stage, illustrated with the stimulation and imaging directions (left) and the stimulation working principle schematics (right), scale bar 8.5 cm
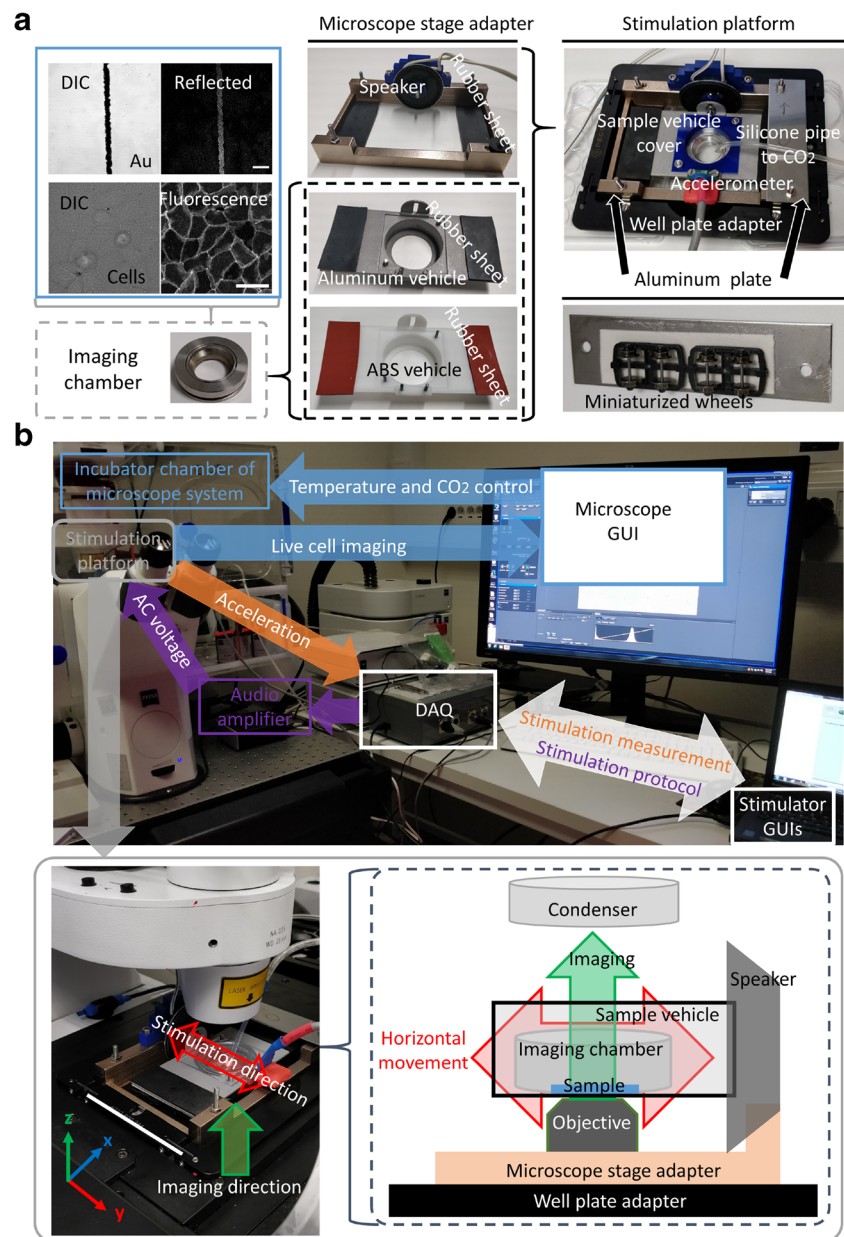
impacts was evaluated. Data extracted from the image was compared with accelerometer data.

2.3 Live cell stimulation experiments

2.3.1 Pre-culture

We investigated compatibility of the stimulation platform for live cell studies by using epithelial cells. Epithelial cells (MDCKII, expressing Emerald-Occludin, highlighting tight-junctions, passage 26) were plated on rattail collagen I - coated (50 μg/ml in 0.2 N Acetic acid, Gibco) coverslips (22 × 22 mm, Carl Zeiss AG). The coverslips were placed on 6-well plates (Thermo Scientific) and cultured inside an

incubator (Steri-Cycle i160, Thermo Scientific) in medium (2 ml; MEM (1X) + GlutaMAX™-I, Gibco; 10% FBS, Gibco; 0.25 mg/ml G418 (geneticin) antibiotic, InvivoGen) until 8–9 days to reach confluence. Fresh medium was changed twice during the pre-culture.

2.3.2 Preparations before stimulation experiment

At the stimulation day, the stimulation platform was placed inside the microscope's incubation system (Incubator XL S1), which was preheated to 37 °C for one hour. The cells were rinsed once with fresh medium, after which the cover glass was mounted into the imaging chamber (Aireka Cells) in imaging medium (600 μl; MEM (1X), no glutamine, no phenol

red, Gibco; 10% FBS, Gibco) (Fig. 1a). The sample temperature was stabilized for 10–15 min inside an incubator (SteriCycle i160), after which it was assembled into the pre-heated stimulation platform. Next, CO_2 concentration from the microscope's incubation system was set to 5% and the sample was connected to the gas exchange (Fig. 1b). Finally, the sample was let to stabilize for 30 min before beginning of the stimulation experiments.

2.3.3 Stimulation experiments

First, to test the compatibility of the experimental setup for live cell studies the sample was imaged from two randomly chosen positions without mechanical stimulation (C-Apochromat 63 × objective/1.20 W Korr M27, z-stack, 67.48 × 67.48 μm) with DIC light and fluorescence light (excitation λ = 488 nm and emission λ = 500–550 nm). These positions were saved for the subsequent imaging of the cellular morphology after every 10–11 min. Each position was imaged with similar imaging settings altogether ten times. Single confocal images of larger areas (134.95 × 134.95 μm) with optimal focal plane were captured in the beginning and after the experiment to ensure that acquisition of the image stacks did not cause excessive bleaching of the Emerald-Occludin.

The samples were then stimulated with the sinusoidal LMHF (0.56 G_{peak}, 30 Hz and 60 Hz) vibration for 8 min to test the mechanical stimulation effects on the epithelial cells. We estimated theoretical movements of the epithelial cells along y-axis during the 30 Hz and 60 Hz HF vibration by calculating peak-to-peak amplitudes of the sinusoidal motion from the 0.56 G_{peak} acceleration. The stimulation bout protocol was repeated ten times. The three-axis acceleration of the aluminum vehicle was recorded in a similar way as when testing the HF vibration performance range. The vibrated samples were imaged after every stimulation bout, as described with the non-stimulated sample.

2.3.4 Data post-processing and analysis

Accuracy and precision of the LMHF vibration during the cell experiments was evaluated from the recorded acceleration data (X Ch, Y Ch, Z Ch) as described previously [31]. In brief, time domain and PSD estimate representations of the sample vehicle movements were determined for eight stimulation bouts of the 30 Hz or 60 Hz frequency vibrations. Mean G_{peak} values were determined from the stimulation bouts to represent G_{peak} values of the LMHF vibration for each movement axis.

The cell culture environment -induced effects on the cellular morphology and tight junctions were evaluated from the confocal microscopy z-stacks after deconvolution (Huygens Essential, Scientific Volume Imaging B.V., Netherlands). To compare the culture duration -dependent Emerald-Occludin localization, the deconvolved z-stacks were converted into maximum intensity projection (MIP) images with Fiji package, after which the brightness and contrast of the MIP images of the individual samples were adjusted identically for all the different time points. A single optimal focal plane was chosen from the DIC z-stack, and this image was processed similarly to the fluorescence light -based MIP images to show the cellular morphology. The larger, single optical section confocal image of the same area was treated correspondingly to the DIC light z-stacks.

3 Results

3.1 Technical performance of the designed stimulation platform

3.1.1 HF vibration ranges of ABS and aluminum vehicles

The designed aluminum and ABS vehicles were easily sterilizable with 70% ethanol (EtOH). The acceleration data showed that the stimulation platform reached even HMHF vibration along the intended main axis movement with both sample vehicles (Fig. 2a). However, the aluminum vehicle reached higher vibration frequencies when compared to the ABS vehicle. Moreover, the ABS vehicle suffered from larger off main axis movement along z-axis when compared to the aluminum vehicle. In contrast, the amount of movement along the x-axis remained notably smaller when compared to the z-axis movement regardless of the sample vehicle. Both sample vehicles produced the sinusoidal HMHF vibration adequately at the vibration frequencies, producing the highest G_{peak} vibration magnitudes (Fig. 2b).

3.1.2 Characterization of the mechanical impact stimuli

Based on the wider performance range of the aluminum vehicle (Fig. 2), we studied the capability of the stimulation platform to produce mechanical impacts with that vehicle. The acceleration data of the sample vehicle movement showed that low magnitude mechanical impacts were produced along the main axis movement direction (y-axis, mean: 0.12–0.14 G_{peak}) with highly varying peak magnitudes (Ratio$_{SD/mean}$: 36–44%) (Fig. 3a). This movement was accompanied with a similar amount of movement along the z-axis (mean: 0.11 G_{peak}), which peak magnitudes were produced more precisely (Ratio$_{SD/mean}$: 9–12%). Movement along the x-axis direction, i.e. the second off main axis, remained only modest (mean: 0.023–0.024 G_{peak}). The blow-up images of the acceleration data showed that only the mechanical impacts produced with the square wave periods were different when compared to the mechanical impacts produced with the sinusoidal and
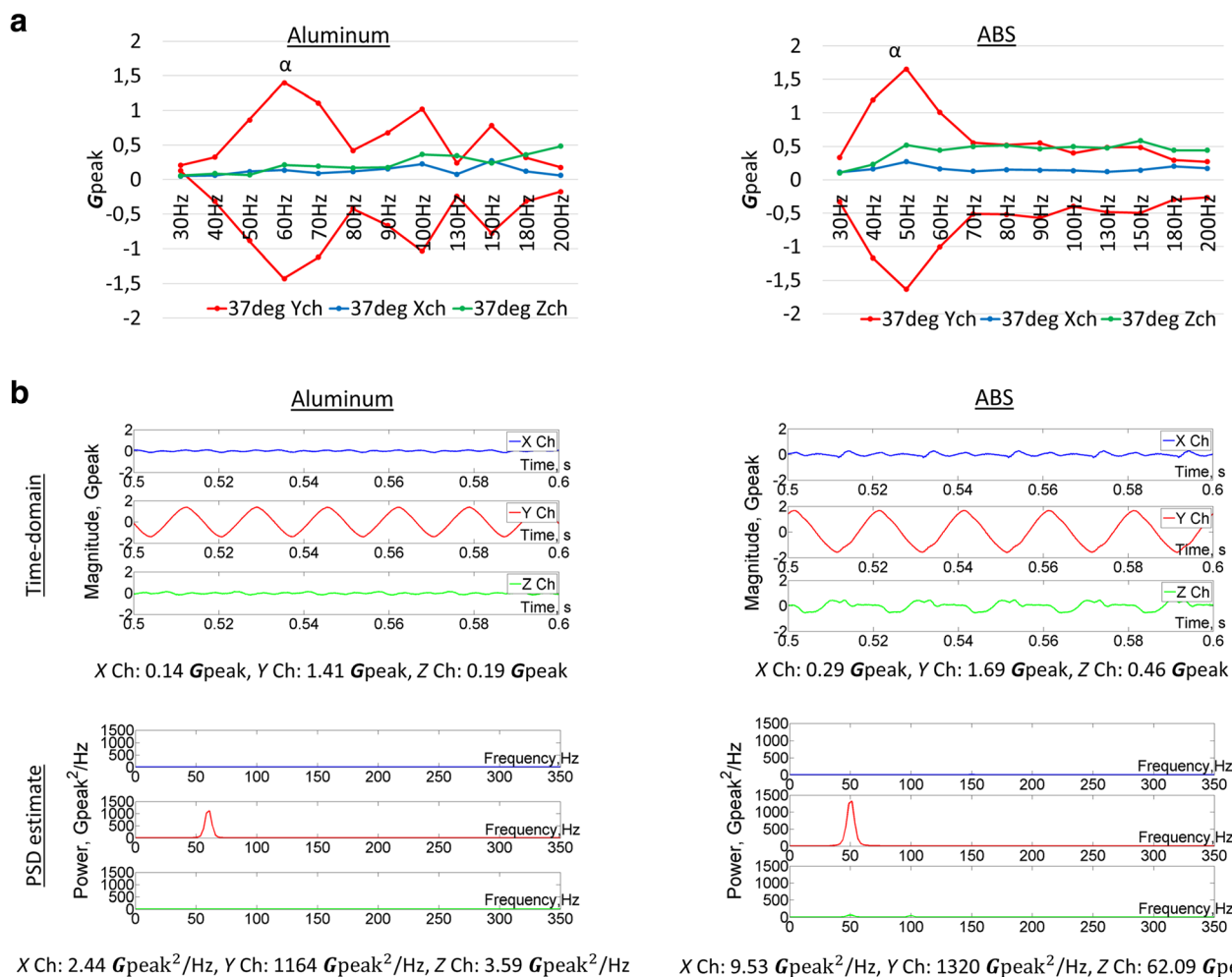
Fig. 2 Summary of the accelerometer -measured HF vibration characteristics of the 3D printed sample vehicles when stimulated with sinusoidal HF vibration (**a**) performance range in 37 °C together with maximum G_{peak} vibration magnitudes (α) of the sample vehicles (**b**) time domain and PSD estimate presentations of the sinusoidal HMHF vibration at the stimulation frequencies corresponding to α magnitudes

triangular wave periods (Fig. 3a, b). The square wave demonstrated at 4/4 T period an extra impact when compared to the 2/4 T period. The AC input signal signs (±) affected the direction of the mechanical impacts.

Time lapse imaging of the Au-printed line showed highly repeatable sample movement during the stimulation protocol, regardless of the mechanical impact parameters (Fig. 4). Changing the AC input voltage reversed the direction of the mechanical impacts, which was confirmed by the acceleration data (Fig. 3b). However, how well the stimulation platform maintained the initial sample position during the stimulation protocol was dependent on the input signal, as demonstrated with the Ratio$_{Last/First}$. Based on blow-up images of the stimulation protocols, the mechanical impacts produced at different periods of sinusoidal wave kept the image field precisely, resulting in most cases in Ratio$_{Last/First}$ of less than 10%. Moreover, with the mechanical impacts produced at the 2/4 T and 4/4 T periods of sine wave the Au-printed line moved slower than at the 1/4 T period, as suggested by the

smoother impact morphologies. The mechanical impacts, produced with the different periods of the triangular wave, resembled morphologically the mechanical impacts produced at the corresponding sine wave periods. Furthermore, they maintained the sample position adequately, as demonstrated with Ratio$_{Last/First}$, which was mostly less than 8%. The steepest curves of the Au-printed line movement were produced with 2/4 T and 4/4 T periods of square wave, demonstrating the fastest movement of the sample. However, Ratio$_{Last/First}$ of even as high as 21–33% with some of the mechanical impacts demonstrated that the sample position was not maintained after the stimulus protocol.

3.2 System performance in live cell stimulation experiments

Experiments with living epithelial cells demonstrated the compatibility of the designed stimulation platform for simultaneous mechanical stimulation and live cell microscopy.
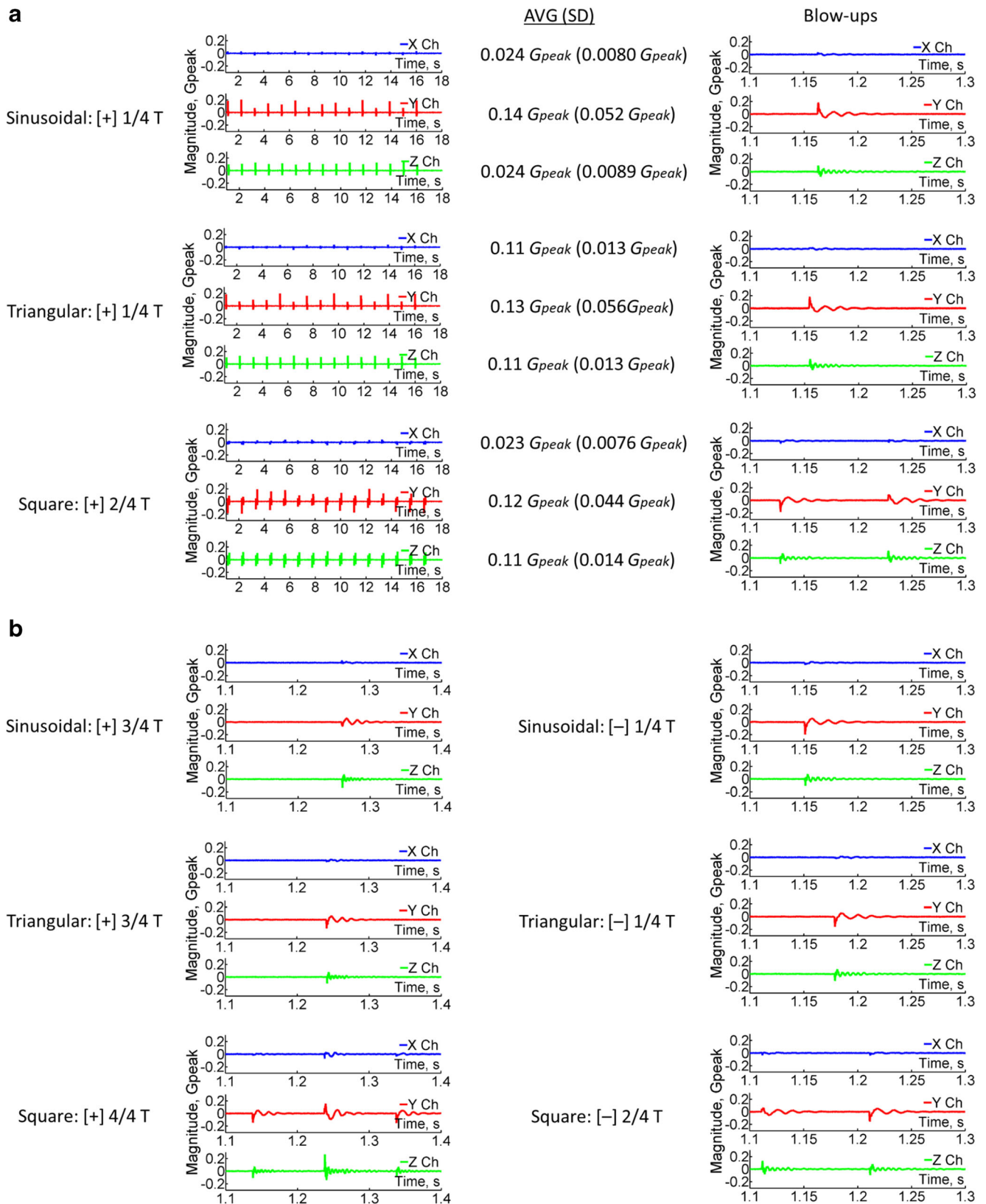
Fig. 3 Visual representations of aluminum vehicle movement as measured with the accelerometer during different mechanical impacts (**a**) accuracy and precision of the mechanical impacts with stimulation protocols, consisting of 14–15 impacts produced with + AC input of 1/4 T periods of sinusoidal and triangular waves and 2/4 T of square wave, combined with their blow-up images (**b**) the blow-up images of the mechanical impacts produced with + AC input of 3/4 T periods of sinusoidal and triangular waves or 4/4 T period of square wave, and mechanical impacts produced with AC input of 1/4 T periods of sinusoidal and triangular waves or 2/4 T period of square wave

Fig. 4 Visual representations of Au-printed line movement during the stimulation protocols, imaged with DIC light during different periods of sinusoidal, triangular and square waves applied either with + or – AC input voltages to determine accuracy and precision of the mechanical impacts (y-axis) together with blow-up images of the mechanical impacts at the initial (First) and the end (Last) positions of the sample combined with their difference, v: $Ratio_{Last/First} < 10\%$, vv: $10\% \leq Ratio_{Last/First} \leq 20\%$, vvv: $Ratio_{Last/First} > 20\%$
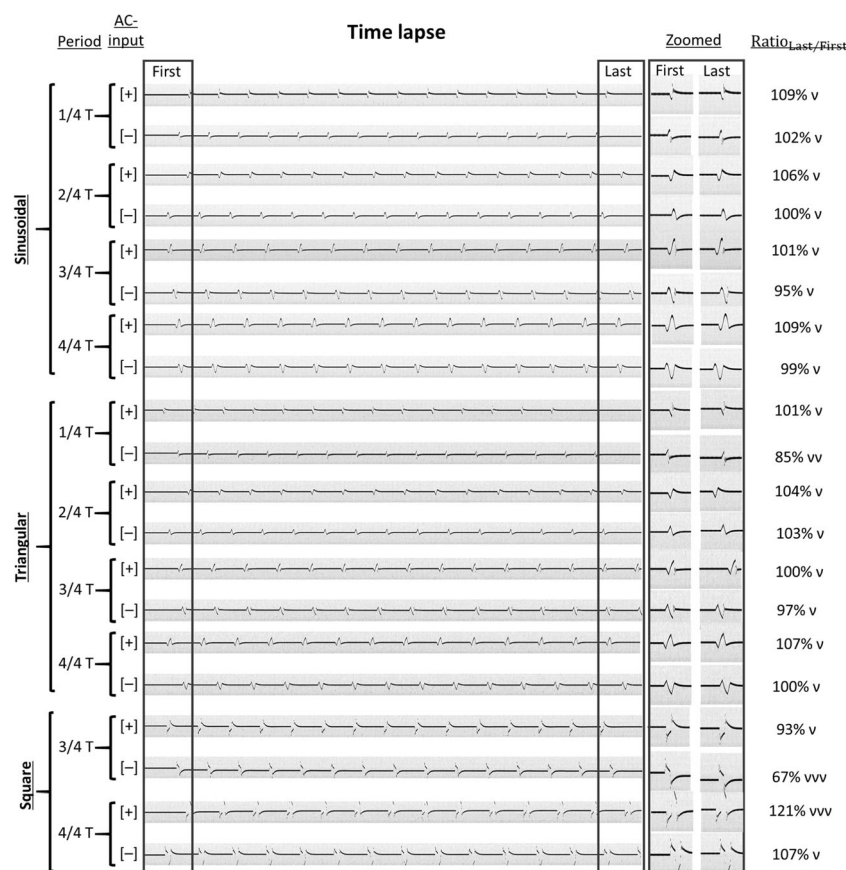
Furthermore, the platform enabled high-resolution imaging of tight junctions of the Emerald-Occludin expressing MDCKII cells. Based on the theoretically calculated maximum displacements of the sample during the LMHF (0.56 G_{peak}, 30 Hz and 60 Hz) vibration, the epithelial cells experienced approximately 290 μm movement at the 30 Hz frequency and approximately 75 μm movement at the 60 Hz frequency. Even as late as at 80 min of the stimulation, no radical changes in the cellular morphology or tight junctions were visible, regardless of the mechanical stimulation (Fig. 5a, b). However, the images taken after the first 8 min of the LMHF vibration demonstrated a sample drift due to the first stimulation bout (Fig. 5b). The drifting was more pronounced at the 30 Hz frequency than at the 60 Hz frequency vibration, but this did not prevent subsequent observation of partially the same image field. Imaging of the larger area at the end of the experiments showed no adverse effects for the cells with the multiple 3D scans of same area (Fig. 5c). Furthermore, the collected accelerometer data showed accurately and precisely produced dynamic mechanical stimuli.

4 Discussion

Currently there is a great need for better tools to investigate cellular mechanobiology and especially the effect of dynamic

mechanical stimulus on cells. Time lapse imaging of living cells provides valuable information of the cellular processes [32–34]. However, combination of live cell microscopy and sample stimulation with mechanical vibration has proven to be difficult. Holdsworth et al. introduced a mechanical stimulation platform, which enables the combined HF vibration and light microscopy of living cells in ambient conditions [30]. We developed the concept further and designed a miniaturized system, which is compatible with the commercial microscope system and its cell culture environment control [31]. In this study, we characterized the system performance in producing HF vibration and impact stimulus. Finally, we tested the compatibility of our system with living cells and imaged epithelial cells, expressing Emerald-Occludin, cultured in the temperature and CO_2 controlled conditions of the microscope. Our findings show that our system is a robust tool for the mechanobiology research, providing the possibility for live cell microscopy between the stimulation bouts or immediately after the dynamic mechanical stimulation.

4.1 Mechanical stimulation platform enables high-resolution light microscopy

The designed stimulation system, consisting both of the stimulation platform and the stimulator GUIs, is user-friendly and

Fig. 5 Representative images of live cell experiments, scale bars 20 μm (**a**) the MDCKII epithelial cells were incubated without dynamic mechanical stimulation in the stimulation platform (37 °C, 5% CO_2) up to 80 min (**b**) the MDCKII epithelial cells were stimulated with 30 Hz and 60 Hz frequency LMHF vibration, stimulation direction illustrated with red arrow (**c**) larger area images of the samples, when imaged at the corresponding positions to **a** and **b**, combined with whisker plots of the LMHF vibration acceleration data collected from stimulation bouts during the experiments
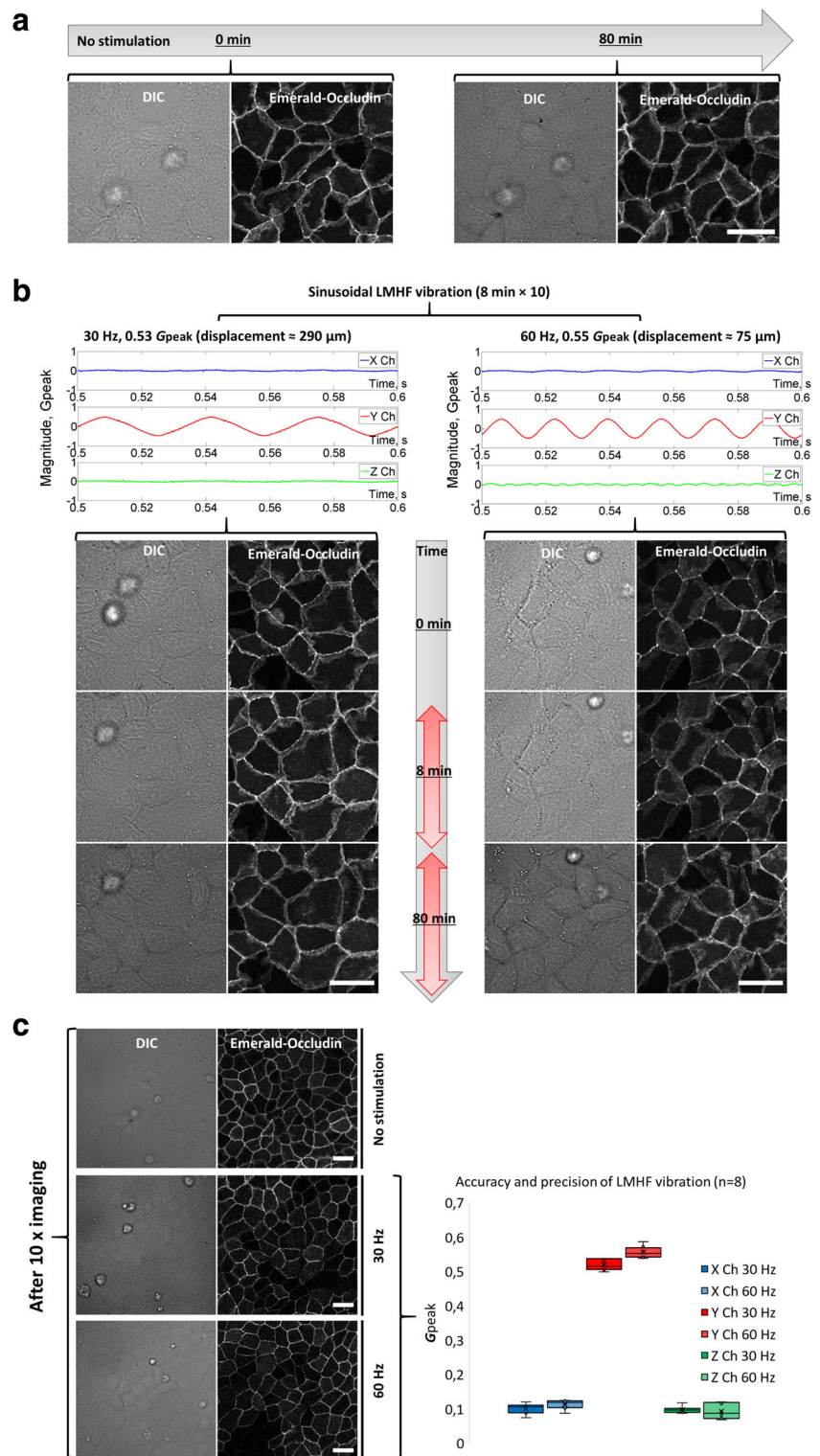
requires only brief training of the user. The system required only little user involvement after assembling the stimulation platform on the microscope stage and after setting the stimulation protocols with the stimulator GUIs, which enabled production of versatile dynamic mechanical stimuli. The acceleration has been used as the most popular determinant of the HF vibration magnitude so far [24, 25], and monitoring and recording of the acceleration data with the stimulator GUIs enables evaluation of the provided mechanical stimulation. Moreover, the miniaturized size makes the system easily

transportable and provides possibility of using the microscope system's own environmental incubation.

According to our previous paper [31], the stimulation platform was able to produce horizontal LMHF vibration at a wide frequency range and the environmental temperature had not considerable effects on the system performance. Consequently, we re-evaluated the HF vibration performance ranges with two different types of sample vehicles only in the cell incubation temperature. We expected that the ABS vehicle, which had a mass less than half of the aluminum vehicle, could reach even higher HF vibration magnitudes or frequencies than the aluminum vehicle. We found in the contrary, the heavier aluminum vehicle reached both higher vibration magnitudes at higher frequencies and covered a wider frequency range when compared to the ABS vehicle. However, the performance of the aluminum vehicle in our current study differs from our previous work performed with the same vehicle [31]. This highlights the importance of proper sample vehicle attachments to the microscope stage adapter and to the speaker, by enabling a stable but frictionless movement. The lighter ABS vehicle suffered from larger movement along the off main axis directions, mainly along the z-axis. However, the modestly higher vibration magnitudes, reached at the lower vibration frequencies, suggest that the lower weight of the ABS vehicle allowed the speaker to move the sample vehicle longer distances when compared to the heavier aluminum vehicle. These differences in the stimulation platform behavior at low and high vibration frequencies can be explained by different mass, and material and structural properties of the sample vehicles affecting for example mechanical resonance. Consequently, different sample vehicles could be used with the different vibration frequencies, with the aim to cover the frequency range more thoroughly. However, stimulating the cells with higher vibration frequencies, referred as nanokicking by Nikukar and colleagues [17], would require replacing of the speaker with an actuator reaching stimulation frequencies up to kHz.

Our platform was designed to produce horizontal stimulation, and to retain the focal plane during the time lapse imaging. In our previous study we demonstrated an excellent fit with the continuously monitored sample movement and the accelerometer-based, calculated displacements of the continuous horizontal HF vibration [31]. However, here the accelerometer-based results of the mechanical impacts demonstrated sample vehicle movements along the z-axis simultaneously with the intended main axis movement. Consequently, this dynamic mechanical stimulus resembles more of the previously introduced stimulation method, applying simultaneously vertical and horizontal HF vibration [19]. This finding suggests that the production of mechanical impacts is more challenging for our stimulation platform than the production HF vibration. Furthermore, time lapse imaging of the Au-printed line allowed us to observe how different mechanical impacts resulted in different sample movement speeds. For the stimulation experiments, in which maintenance of the image field is of high importance, the most suitable option

of the mechanical impacts are sinusoidal wave periods. However, when the high speed of the mechanical impacts is more preferable, then square wave should be used to produce the mechanical impacts. Our current findings with the mechanical impacts, together with our previous findings with the HF vibration [31], suggest that the reliable evaluation of the produced mechanical impacts, but not of the HF vibration, requires both the accelerometer and the time lapse imaging data.

4.2 Applicability for mechanobiology research with live cells

The HF vibration has been especially popular in inducing the osteogenic responses of stem cells [9–11, 35] and in differentiation of the vocal fold tissues [16]. However, these stimulation effects have been studied with methods, which require special treatments of the samples and don't allow live cell imaging. Time lapse imaging and different mechanical manipulation of living cells have been recently used to study cellular responses either to the stretching [33] or to the combination of the atomic force microscopy and traction force microscopy [34]. In our previous study, we demonstrated that our stimulation platform maintains the image field allowing almost real-time imaging of the cellular responses to the LMHF vibration with high-resolution light microscopy [31]. Here, we demonstrate that our system provides also sufficient cell culture conditions at least for up to 2 h when combined with a proper environmental control.

Consequently, we could test the LMHF vibration effects on the cellular morphology and tight junctions of the epithelial cells. Our current findings with the DIC and fluorescence images of the Emerald-Occludin expressing MDCKII cells show our system has a great potential for the quantitative analysis of label free and fluorescence -based imaging. The minor sample drift after the mechanical stimulation can be overcome by imaging larger fields with microscope or moving the imaged area accordingly after the first stimulation bout. Interestingly, our initial findings suggest no radical changes in tight junctions or morphology of the epithelial cells even after 80 min of stimulation. The epithelial cells seem to tolerate the LMHF vibration well, whereas the cells rapidly respond to the mechanical stretching [26, 27]. This suggests a need to test also different stimulation parameters of the HF vibration.

4.3 Device performance limitations and future improvement suggestions

Our high-resolution light microscopy -compatible stimulation platform enables combining of different biochemical cues with mechanical manipulation of the cellular niche in 2D or in thin and transparent 3D samples. As a result, the device enables to obtain more detailed information of the stimulus effects on the mechanocoupling sites of the HF vibration [18, 36]. Currently, the tool enables to obtain data simultaneously

from several cells, but the actual sample number renders still relatively low because the sample vehicle accepts only a single imaging chamber at a time. This drawback could be solved with 3D printing of a new sample vehicle, accepting commercial multiwell chambered coverslips that have been introduced for the light microscopy imaging [37]. However, performing the experiments with these multiwell platforms would also reduce temporal resolution of the microscopy, due to the need of sample movement and refocusing. This should be considered, when studying any functional responses of the cells for which both spatial and temporal data are important. The stimulation platform enables for example studying of rapid electrophysiological responses, such as Ca^{2+} signaling which is involved to several cellular processes [38].

With our simple sample cover, we could use the temperature and CO_2 controls of the confocal microscopy system, regardless that the height of the speaker prevented us from using the confocal microscopy system's own small incubation chamber. This allowed us to perform cell experiments at the microscope system up to a few hours. However, when using our stimulation platform at the microscope systems without the environmental controls, a miniaturized and a portable cell incubation device would be needed [39]. Another limitation with the current experimental setup is also time-taking preheating and stabilization of the microscope system and the sample, which limits the sample number only to a few samples per day, depending on the stimulus protocol. This drawback could be solved by adding a custom-made heating system [40] to the sample vehicle to control the temperature in the proximity of the sample more robustly and efficiently.

Our live cell experiments demonstrated that our system enables imaging of cellular response to the LMHF vibration, but the initial findings with epithelial cells suggest that more rapid and intense changes in the epithelial cell morphology requires different vibration parameters. To meet more comprehensively the varying stimulation needs of different cellular application areas, the sample should be moved at higher frequencies and with larger vibration magnitudes. This would require both replacing the current speaker with a proper actuator and optimizing the structural and material properties of the stimulation platform. In the future, our stimulation platform enables studies of mechanotransduction-based processes in living cells, which is important for further understanding on how mechanical stimulation can influence cellular physiology.

5 Conclusions

Currently there are only limited number of tools to study mechanotransduction in vitro. To meet this limitation, we developed a device for mechanobiological research which combines simultaneous mechanical stimulation (HF vibration or mechanical impacts) and high-resolution light microscopy of the living cells. The system, consisting of two different sample vehicles and software, was capable of sufficiently covering the usual stimulation parameters of different HF vibration cell studies, but also producing of novel impact-like mechanical stimuli. The mechanical impacts were most accurately produced by varying periods of the sinusoidal wave. Our findings with the epithelial cells show that the designed system is compatible with live cell experiments. The microscope image field drifted only short distances during several stimulation bouts, allowing us to study cellular response to the LMHF vibration. During the relatively short stimulation experiments, we were not able to detect any major changes in epithelial cell morphology. Thus, the effects of the HF vibration and the mechanical impacts on the epithelial mechanobiology remain to be studied. Long-term experiments with living cells will require also a more sophisticated control of the incubation conditions (temperature and CO_2). These studies will deepen our understanding on the effects of the HF vibration and mechanical impact stimuli on cells that is required before the methodology can be utilized more widely in different cellular applications.

Ethical approval This article does not contain any studies with human participants or animals performed by any of the authors.

Statements of informal consent Informed consent was obtained from all individual participants included in this study.

Compliance with ethical standards

Conflict of interest The authors declare no conflicts of interest.

References

1. Orr AW, Helmke BP, Blackman BR, Schwartz MA. Mechanisms of Mechanotransduction. Dev Cell. 2006;10:11–20.
2. Vainionpää A, Korpelainen R, Vihriälä E, Rinta-Paavola A, Leppäluoto J, Jämsä T. Intensity of exercise is associated with bone

density change in premenopausal women. Osteoporos Int. 2006;17: 455–63.

3. Califano JP, Reinhart-King CA. Exogenous and endogenous force regulation of endothelial cell behavior. J Biomech. 2010;43: 79–86.

4. Wang NW, Tytell JD, Ingber DE. Mechanotransduction at a distance: mechanically coupling the extracellular matrix with the nucleus. Nat Rev Mol Cell Biol. 2009;10:75–82.

5. Martino F, Perestrelo AR, Vinarsky V, Pagliari S, Forte G. Cellular Mechanotransduction: from tension to function. Front Physiol. 2018;9:824.

6. Evans ND, Oreffo RO, Healy E, Thurner PJ, Man YH. Epithelial mechanobiology, skin wound healing, and the stem cell niche. J Mech Behav Biomed Mater. 2013;28:397–409.

7. Hsu CK, Lin HH, Harn HI, Hughes MW, Tang MJ, Yang CC. Mechanical forces in skin disorders. J Dermatol Sci. 2018;90: 232–40.

8. Zhang Z. Mechanics of human voice production and control. J Acoust Soc Am. 2016;140:2614–35.

9. Tirkkonen L, Halonen H, Hyttinen J, Kuokkanen H, Sievänen H, Koivisto AM, et al. The effects of vibration loading on adipose stem cell number, viability and differentiation towards bone-forming cells. J R Soc Interface. 2011;8:1736–47.

10. Uzer G, Pongkitwitoon S, Ete Chan M, Judex S. Vibration induced osteogenic commitment of mesenchymal stem cells is enhanced by cytoskeletal remodeling but not fluid shear. J Biomech. 2013;46: 2296–302.

11. Kim IS, Song YM, Lee B, Hwang SJ. Human Mesenchymal stromal cells are Mechanosensitive to vibration stimuli. J Dent Res. 2012;91:1135–40.

12. Choi YK, Cho H, Seo YK, Yoon HH, Park JK. Stimulation of subsonic vibration promotes the differentiation of adipose tissue-derived mesenchymal stem cells into neural cells. Life Sci. 2012;91:329–37.

13. Wu SH, Zhong ZM, Chen JT. Low-magnitude high-frequency vibration inhibits RANKL-induced osteoclast differentiation of RAW264.7 cells. Int J Med Sci. 2012;9:801–7.

14. Zhao Q, Lu Y, Gan X, Yu H. Low magnitude high frequency vibration promotes adipogenic differentiation of bone marrow stem cells via P38 MAPK signal. PLoS One. 2017;12:e0172954.

15. Takeuchi E, Saito T, Ishikawa H, Takigami H, Dezawa M, Ide C, et al. Effects of vibration and hyaluronic acid on activation of three-dimensional cultured chondrocytes. Arthritis Rheum. 2006;54: 1897–905.

16. Kutty JK, Webb K. Vibration stimulates vocal mucosa-like matrix expression by hydrogel-encapsulated fibroblasts. J Tissue Eng Regen Med. 2010;4:62–72.

17. Nikukar H, Reid S, Tsimbouri PM, Riehle MO, Curtis AS, Dalby MJ. Osteogenesis of mesenchymal stem cells by nanoscale mechanotransduction. ACS Nano. 2013;7:2758–67.

18. Uzer G, Manske SL, Chan ME, Chiang FP, Rubin CT, Frame MD, et al. Separating fluid shear stress from acceleration during vibration in vitro: identification of mechanical signals modulating the cellular response. Cell Mol Bioeng. 2012;5:266–76.

19. Pré D, Ceccarelli G, Gastaldi G, Asti A, Saino E, Visai L, et al. The differentiation of human adipose-derived stem cells (hASCs) into osteoblasts is promoted by low amplitude, high frequency vibration treatment. Bone. 2011;49:295–303.

20. Gaston J, Rios BQ, Bartlett R, Berchtold C, Thibeault SL. The response of vocal fold fibroblasts and Mesenchymal stromal cells to vibration. PLoS One. 2012;7:e30965.

21. Dumas V, Perrier A, Malaval L, Laroche N, Guignandon A, Vico L, et al. The effect of dual frequency compression on matrix deposition by osteoblast-like cells grown in 3D scaffolds and on modulation of VEGF variant expression. Biomaterials. 2009;30:3279–88.

22. Lorusso D, Nikolov HN, Chmiel T, Beach RJ, Sims SM, Dixon SJ, Holdsworth DW. A device for real-time live-cell microscopy during dynamic dual-modal mechanostimulation. In: Krol A, Gimi B, editors. Medical Imaging 2017: Biomedical Applications in Molecular, Structural, and Functional Imaging, Proceedings of SPIE, vol. 10137. SPIE; 2017. pp. 101370F-1–101370F-7.

23. Sen B, Xie Z, Case N, Styner M, Rubin CT, Rubin J. Mechanical signal influence on mesenchymal stem cell fate is enhanced by incorporation of refractory periods into the loading regimen. J Biomech. 2011;44:593–9.

24. Edwards JH, Reilly GC. Vibration stimuli and the differentiation of musculoskeletal progenitor cells: review of results in vitro and in vivo. World J Stem Cells. 2015;7:568–82.

25. McClarren B, Olabisi R. Strain and vibration in Mesenchymal stem cells. Int J Biomater. 2018;8686794.

26. Benham-Pyle BW, Pruitt BL, Nelson WJ. Cell adhesion. Mechanical strain induces E-cadherin–dependent Yap1 and β-catenin activation to drive cell cycle entry. Science. 2015;348: 1024–7.

27. Hart KC, Tan J, Siemers KA, Sim JY, Pruitt BL, Nelson WJ, et al. E-cadherin and LGN align epithelial cell divisions with tissue tension independently of cell shape. PNAS. 2017:E5845–53.

28. Duan Y, Gotoh N, Yan Q, Du Z, Weinstein AM, Wang T, et al. Shear-induced reorganization of renal proximal tubule cell actin cytoskeleton and apical junctional complexes. Proc Natl Acad Sci U S A. 2008;105:11418–23.

29. Maggiorani D, Dissard R, Belloy M, Saulnier-Blache J-S, Casemayou A, Ducasse L, et al. Shear stress-induced alteration of epithelial Organization in Human Renal Tubular Cells. PLoS One. 2015;10:e0131416.

30. Holdsworth DW, Nikolov HN, Au J, Beaucage K, Kishimoto J, Dixon SJ. Simultaneous vibration and high-speed microscopy to study mechanotransduction in living cells. In: Molthen RC, Weaver JB, editors. Medical Imaging 2012: Biomedical Applications in Molecular, Structural, and Functional Imaging, Proceedings of SPIE, vol. 8317. SPIE; 2012. pp. 831715–1–831715-6.

31. Halonen H, Hyttinen JAK, Ihalainen TO. Miniaturized stimulator for imaging of live cell responses to high frequency mechanical vibration. In: Badnjevic A, Skribic R, Gurbeta PL, editors. CMBEBIH 2019. IFMBE proceedings, vol. 73. Cham: Springer; 2020. p. 21–7.

32. Piltti KM, Cummings BJ, Carta K, Manughian-Peter Ayla, Worne CL, Singh K, Ong D, Maksymyuk Y, Khine M, Anderson AJ. Live-cell time-lapse imaging and single-cell tracking of in vitro cultured neural stem cells – Tools for analyzing dynamics of cell cycle, migration, and lineage selection. Methods. 2018;133:81–90.

33. Bianchi F, Pereno V, George JH, Thompson MS, Ye H. Membrane mechanical properties regulate the effect of strain on spontaneous electrophysiology in human iPSC-derived neurons. Neuroscience. 2019;404:165–74.

34. Schierbaum N, Rheinlaender J, Schäffer TE. Combined atomic force microscopy (AFM) and traction force microscopy (TFM) reveals a correlation between viscoelastic material properties and contractile prestress of living cells. Soft Matter. 2019;15:1721–9.

35. Pongkitwitoon S, Uzer G, Rubin J, Judex S. Cytoskeletal configuration modulates mechanically induced changes in Mesenchymal stem cell Osteogenesis, morphology, and stiffness. Sci Rep. 2016;6: 34791.

36. Uzer G, Thompson WR, Sen B, Xie Z, Miller SS, Bas G, et al. Cell Mechanosensitivity to extremely low-magnitude signals is enabled by a LINCed nucleus. Stem Cells. 2015;33:2063–76.

37. Virant D, Traenkle B, Maier J, Kaiser PD, Bodenhöfer M, Schmees C, et al. A peptide tag-specific nanobody enables high-quality labeling for dSTORM imaging. Nat Commun. 2018;90:930.

38. Clapham DE. Calcium signaling. Cell. 2007;131:1047–58.

39. Kreutzer J, Ylä-Outinen L, Mäki AJ, Ristola M, Narkilahti S, Kallio P. Cell culture chamber with gas supply for prolonged recording of human neuronal cells on microelectrode array. J Neurosci Methods. 2017;280:27–35.

40. Mäki AJ, Verho J, Kreutzer J, Ryynänen T, Rajan D, Pekkanen-Mattila M, et al. A portable microscale cell culture system with indirect temperature control. SLAS Technol. 2018;1: 2472630318768710.